Electronic Supplementary Information

Oxygen reduction catalyzed by a water-soluble binuclear copper(II) complex from a neutral aqueous solution

Chengyu Liu,[a] Haitao Lei,[a] Zongyao Zhang,[a] Fangfang Chen,[b] and Rui Cao*[ab]

[a]Department of Chemistry, Renmin University of China, Beijing 100872 China.

[b]School of Chemistry and Chemical Engineering, Shaanxi Normal University, Xi'an 710119 China.

*Correspondence E-mail: ruicao@ruc.edu.cn

General Methods and Materials.

Manipulations of air- and moisture-sensitive materials were performed under nitrogen using standard Schlenk line techniques. Unless otherwise noted, all reagents and solvents were purchased from commercial suppliers and were used without further purification. Organic solvents were distilled prior to use. Water was deionized and purified by passing through a Labconco WaterPros water purification system. Complexes **2**[1] and **3**[2] were synthesized according to literature reports. The ^{1}H NMR and ^{13}C NMR measurements were made on a Brüker spectrometer operating at 400 and 600 MHz, respectively. High-resolution mass spectra were acquired on a Brüker Fourier Transform Ion Cyclotron Resonance Mass Spectrometer APEX IV. UV-vis spectra were obtained using a Hitachi U-3310 spectrophotometer.

Synthesis and Characterization.

Synthesis of polypyridine-polyamide ligand L: The new five-coordinated polypyridine-polyamide ligand **L** was synthesized according to the synthetic route depicted in Scheme S1.

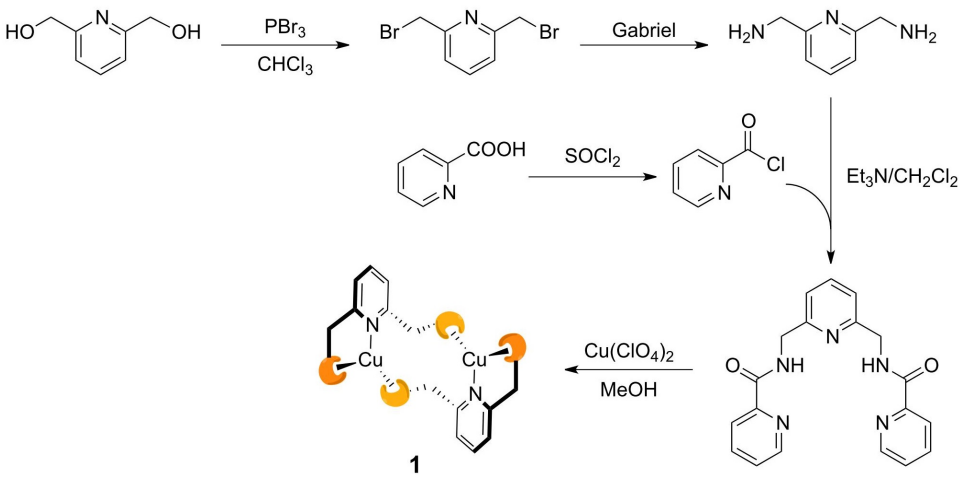

Scheme S1. Synthetic route of ligand **L** and complex **1**.

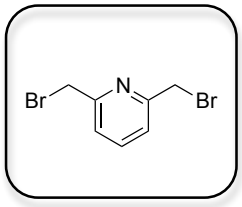

Synthesis of 2,6-dibromomethylpyridine. To a stirred solution of 2,6-pyridinedimethanol (2.0 g, 14.4 mmol) in $CHCl_3$ (20 mL) in an ice-bath, PBr_3 (1.36 mL, 14.4 mmol) was dropwise added. The resulted solution was refluxed for 18 h, cooled to room temperature, and was then quenched by H_2O (20 mL). The mixture solution was extracted by $CHCl_3$ (30 mL) three times. The combined organic layer was washed by saturated NaCl aqueous solution, dried over Na_2SO_4. The product was collected by rotary evaporation to give a white solid (2.36 g, 62% yield). ^{1}H NMR (400 MHz, $CDCl_3$): δ = 7.71 (t, J = 7.8 Hz, 1H), 7.38 (d, J = 7.8 Hz, 2H), 4.55 (s, 4H) (Fig. S2); ^{13}C NMR (600 MHz, $CDCl_3$): δ = 33.6, 122.8, 138.2, 156.6 (Fig. S3); High resolution mass spectrometry: calcd. for [$C_7H_7Br_2N+H^+$]: 263.9023; found, 263.9008 (Fig. S4).

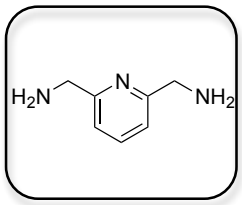

Synthesis of 2,6-diaminomethylpyridine. A stirred mixture of 2,6-dibromomethylpyridine (2.36 g, 8.9 mmol) and potassium phthalimide (3.30 g, 17.8 mmol) in DMF (10 mL) was heated to 100 °C for 48 h. H_2O (20 mL) was added after the solution was cooled to room temperature. The resulting white solid was collected by filtration, dispersed into ethyl alcohol (20 mL), and the mixture was then refluxed for 24 h after adding hydrazine hydrate (1.67 mL). The solution was cooled to room temperature, followed by the addition of 6 M HCl (20 mL), and was then refluxed for 2 h, and was stirred at room temperature for additional 10 h. After filtration, the filtrate was added 6 M KOH solution. The water layer was extracted by $CHCl_3$ for three times, and the organic layer was collected, dried over Na_2SO_4. The light brown solid product (0.92 g, 75% yield) was collected by rotary evaporation after filtration. ^{1}H NMR (400 MHz, $CDCl_3$): δ = 7.57 (t, *J* = 7.8 Hz, 1H), 7.10 (d, *J* = 7.8 Hz, 2H), 3.93 (s, 4H), 1.81 (brs, 4H) (Fig. S5); ^{13}C NMR (600 MHz, $CDCl_3$): δ = 47.6, 119.1, 136.9, 161.3 (Fig. S6); High resolution mass spectrometry: calcd. for [$C_7H_{11}N_3$+H^+]: 138.1031; found, 138.1021 (Fig. S7).

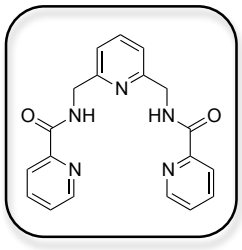

*Synthesis of ligand **L***. A stirred solution of pyridine-2-carboxylic (1.65 g, 13.4 mmol) in $SOCl_2$ (20 mL) was refluxed for 6 h, and was then cooled to room temperature. The organic solvent was evaporated before adding triethylamine (8 mL) and dichloromethane (12 mL) under N_2 atmosphere. To this solution, 2,6-diaminomethylpyridine (0.92 g, 6.7 mmol) was

added, and the solution was stirred at room temperature for 24 h. The organic solvent was then washed three times using saturated NaCl aqueous solution and water, and was separated and dried over Na_2SO_4. The crude product was collected by rotary evaporation after filtration and purified by re-crystallization using absolute methanol to give a white solid (1.63 g, 70% yield). ^{1}H NMR (400 MHz, $CDCl_3$): δ = 8.95 (brs, 2H), 8.54 (d, *J* = 4.6 Hz, 2H), 8.25 (d, *J* = 7.8 Hz, 2H), 7.89 (t, *J* = 7.8 Hz, 2H), 7.68 (t, *J* = 7.6 Hz, 1H), 7.48 (q, *J* = 7.8 Hz, *J* = 4.6 Hz, 2H), 7.29 (d, *J* = 7.6 Hz, 2H), 4.88 (d, *J* = 5.9 Hz, 4H) (Fig. S8); ^{13}C NMR (600 MHz, $CDCl_3$): δ = 44.6, 122.3, 123.1, 126.2, 137.2, 137.3, 148.2, 149.8, 156.7, 164.5 (Fig. S9); High resolution mass spectrometry: calcd. for [$C_{19}H_{17}N_5O_2$+H^+]: 348.1460; found, 348.1440 (Fig. S10).

Synthesis of complex 1: A mixture solution of ligand **L** (1.63 g, 4.7 mmol) and $Me_4N(OH)$ (0.85 g, 9.4 mmol) in absolute methanol (160 mL) was stirred for 10 min. $Cu(ClO_4)_2$ (1.23 g, 4.7 mmol) was then added, and the solution was stirred at room temperature for 6 h. The resulted suspension was filtered, the organic solvent was evaporated, and the residue was re-dissolved in water. Slow evaporation at room temperature gave complex **1** as blue-green crystals (1.34 g, 70% yield). Anal. calcd for [$C_{38}H_{30}Cu_2N_{10}O_4$]: C, 55.81; H, 3.70; N, 17.13. Found: C, 55.51; H, 3.90; N, 16.83. High resolution mass spectrometry: calcd. for [$C_{38}H_{30}Cu_2N_{10}O_4$]: 816.1043; found, 816.1068 (Fig. S11).

Electrochemistry.

CV measurements were performed using a CH Instruments (model CHI660D Electrochemical Analyzer). CV recorded in DMF solutions (0.1 M Bu_4NPF_6) used a three compartment cell possessing a 0.07 cm^2 GC electrode as the working electrode, Pt wire as the auxiliary electrode, and $Ag/AgNO_3$ as the reference electrode (BASi, 10 mM $AgNO_3$, 0.1 M Bu_4NPF_6 in DMF). Ferrocene was added at the end of the measurement as an internal standard. In aqueous solvents, Ag/AgCl (KCl-saturated) was used as the reference electrode, and the potential was converted relative to NHE. Unless otherwise indicated, the CV scan rate was 50 mV s^{-1} in both organic and aqueous solvents. For experiments conducted with or without O_2, the solutions were bubbled with high-purity O_2 or N_2 for at least 30 min before analysis. For RRDE measurements, a bipotentiostat (model DY2300 Electrochemical Analyzer) and a rotating ring-disk electrode with a rotating GC disk electrode (4 mm diameter) and a Pt ring electrode (ALS RRDE-2) were used. The collection efficiency of the ring-disk electrode was evaluated using the $[Fe(CN)_6]^{3-/4-}$ redox couple and was calculated to be 0.468.

X-ray Diffraction Studies.

Complete data set for complex **1** (CCDC 1516460) was collected. Single crystal suitable for X-ray analysis was coated with Paratone-N oil, suspended in a small fiber loop, and placed in a cold gaseous nitrogen stream on a Bruker D8 VENTURE X-ray diffractometer performing ϕ- and ω-scans at 150(2) K. Diffraction

intensities were measured using graphite monochromated Mo *K*α radiation (λ = 0.71073 Å). Data collection, indexing, initial cell refinements, frame integration, and final cell refinements were accomplished using the program APEX2.[3] Absorption corrections were applied using SADABS.[4] Scattering factors and anomalous dispersion corrections were taken from the *International Tables for X-ray Crystallography*. All structures were solved by direct methods using SHELXS[5] and refined against F^2 on all data by full-matrix least squares with SHELXL[6] following established refinement strategies.

In the structure of **1**, all non-hydrogen atoms were refined anisotropically. All hydrogen atoms binding to carbon were included into the model at geometrically calculated positions and refined using a riding model. The isotropic displacement parameters of all hydrogen atoms were fixed to 1.2 times the U value of the atoms they are linked to. Details of the data quality and a summary of the residual values for the refinements are listed in Table S1.

Calculation of *n* value.

The *n* value calculated using the RRDE data:

$$n = \frac{4 i_{disk}}{i_{disk} + \frac{i_{ring}}{N_{eff}}}$$

in which i_{disk} is the disk current, i_{ring} is the ring current, and N_{eff} = 0.468 is the collection efficiency evaluated using the $[Fe(CN)_6]^{3-/4-}$ redox couple.

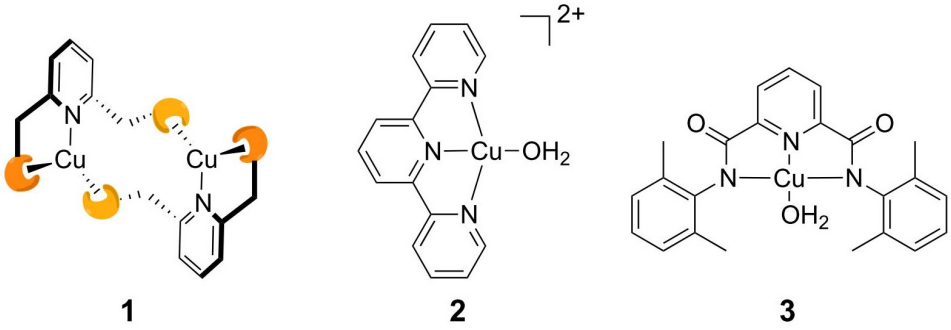

1 2 3

Figure S1. Molecular structures of complexes **1**, **2**, and **3**.

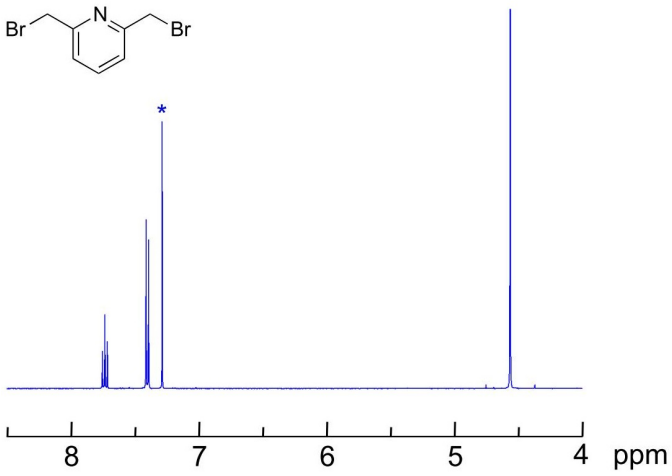

Figure S2. ^{1}H NMR spectrum of 2,6-dibromomethylpyridine in $CDCl_3$.

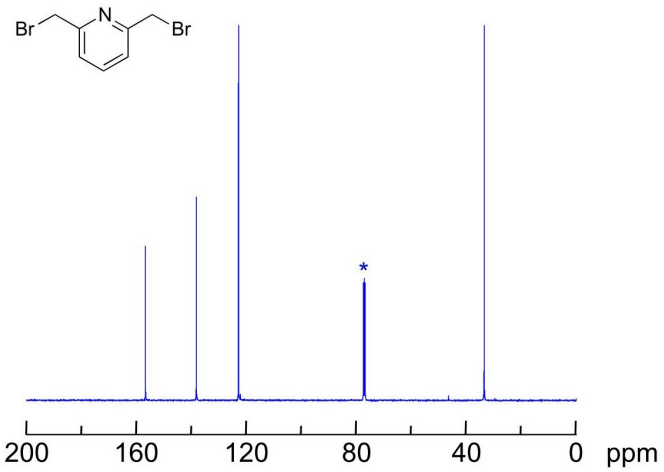

Figure S3. ^{13}C NMR spectrum of 2,6-dibromomethylpyridine in $CDCl_3$.

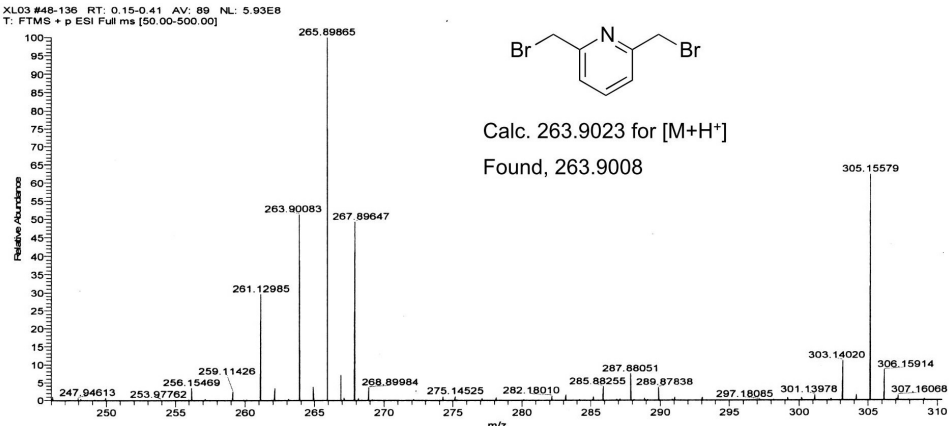

Figure S4. HRMS of 2,6-dibromomethylpyridine in methanol. The observed isotopic distribution pattern is identical to that calculated using the formula [$C_7H_7Br_2N$].

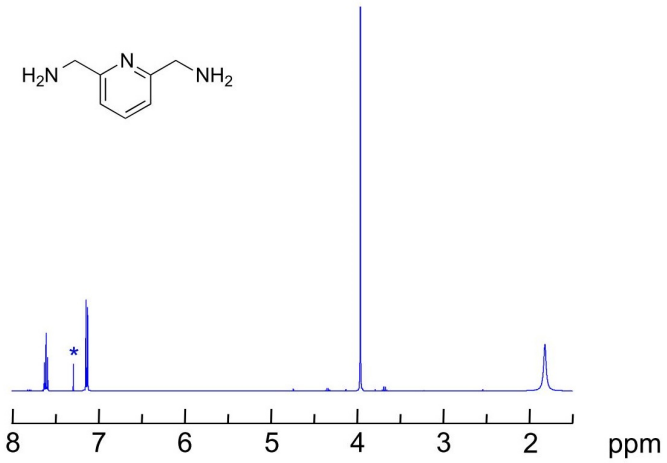

Figure S5. ^{1}H NMR spectrum of 2,6-diaminomethylpyridine in $CDCl_3$.

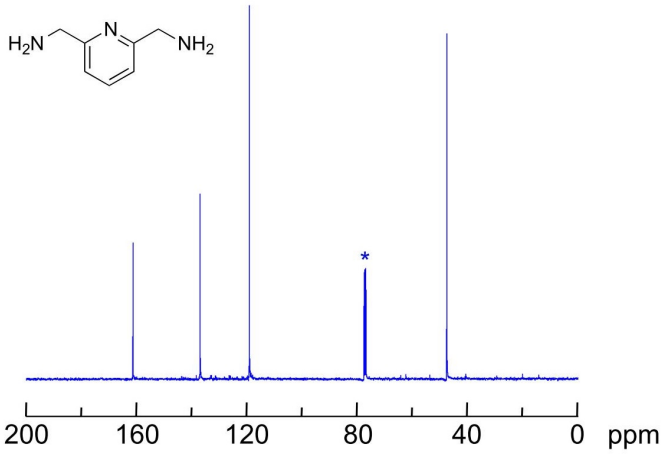

Figure S6. ^{13}C NMR spectrum of 2,6-diaminomethylpyridine in $CDCl_3$.

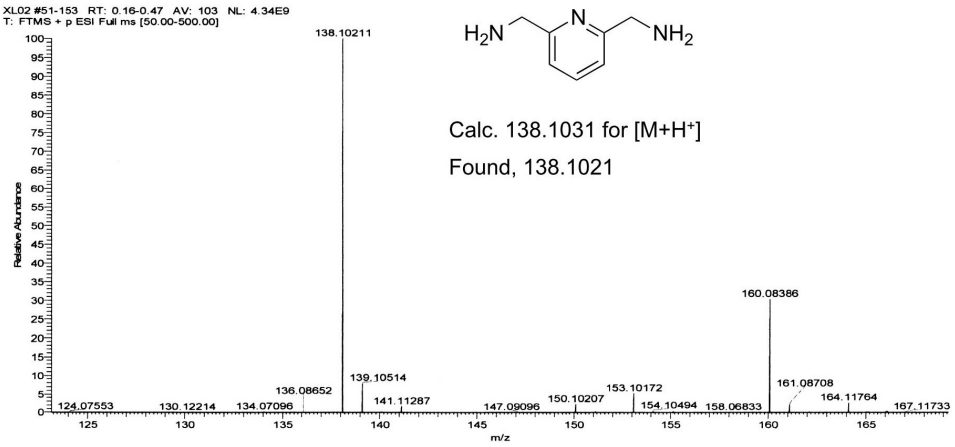

Figure S7. HRMS of 2,6-diaminomethylpyridine in methanol. The observed isotopic distribution pattern is identical to that calculated using the formula [$C_7H_{11}N_3$].

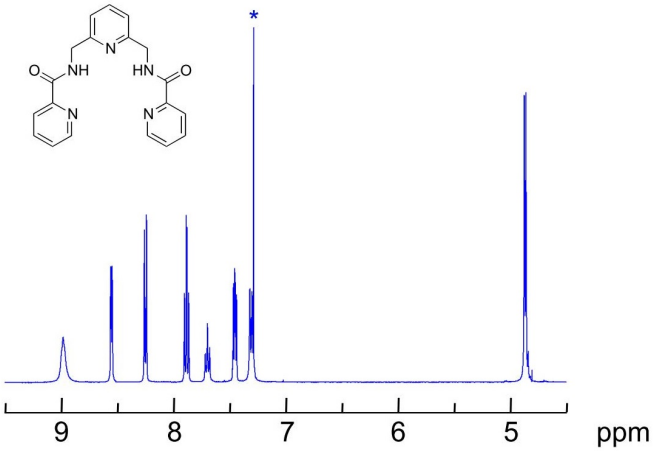

Figure S8. ^{1}H NMR spectrum of ligand **L** in $CDCl_3$.

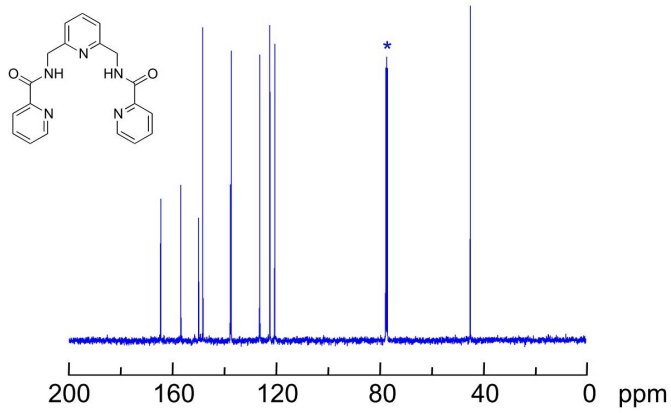

Figure S9. ^{13}C NMR spectrum of ligand **L** in $CDCl_3$.

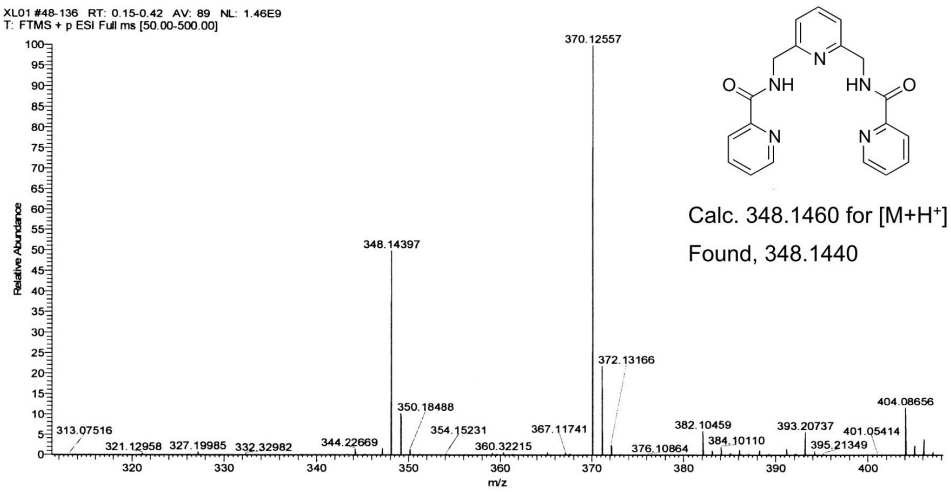

Figure S10. HRMS of ligand **L** in methanol. The observed isotopic distribution pattern is identical to that calculated using the formula [$C_{19}H_{17}N_5O_2$].

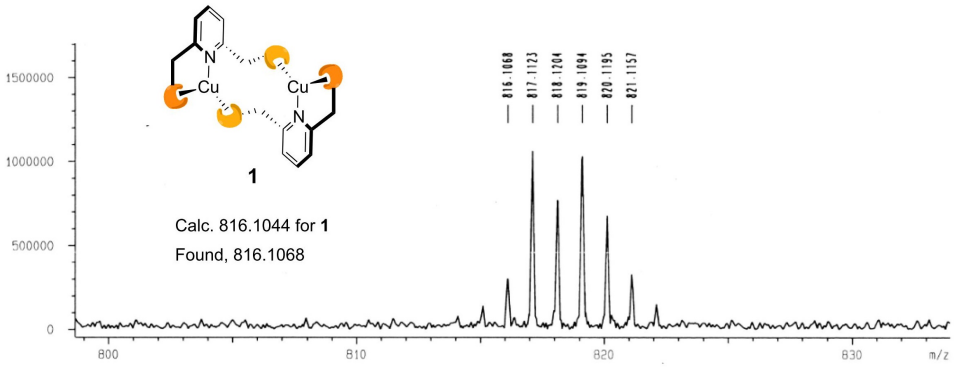

Figure S11. HRMS of complex **1** in methanol. The observed isotopic distribution pattern is identical to that calculated using the formula $[C_{38}H_{30}Cu_2N_{10}O_4]$.

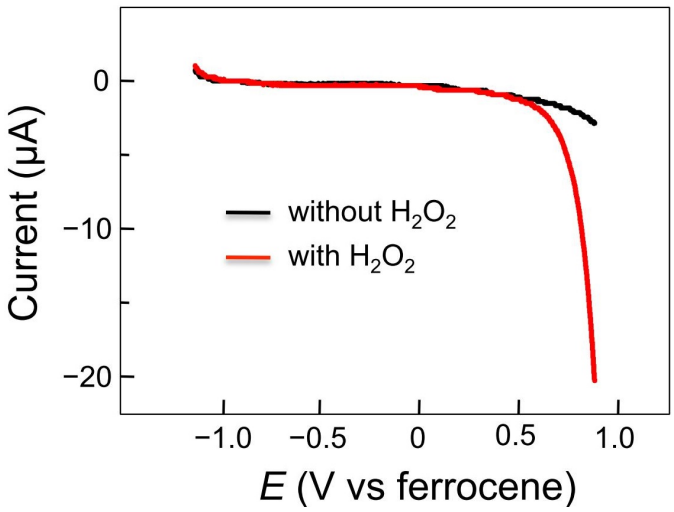

Figure S12. LSVs of DMF solutions with or without 10.0 mM of H_2O_2 on Pt ring electrode. Conditions: Pt ring (area 0.188 cm^2), 50 mV s^{-1} scan rate, 20 °C.

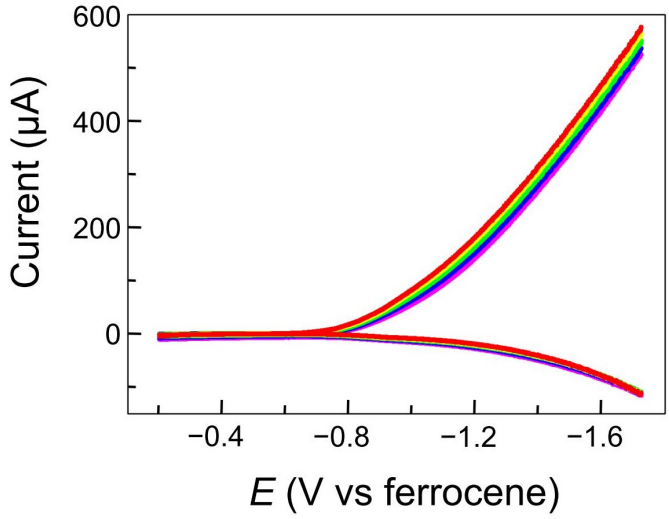

Figure S13. RRDE measurements of 0.1 mM **1** in DMF under O_2 after adding 170-510 mM of acetic acid. Conditions: 0.7 V (vs ferrocene) ring potential, GC disk (area 0.125 cm^2), Pt ring (area 0.188 cm^2), 50 mV s^{-1} scan rate, 2500 rpm rotation rate, 20 °C.

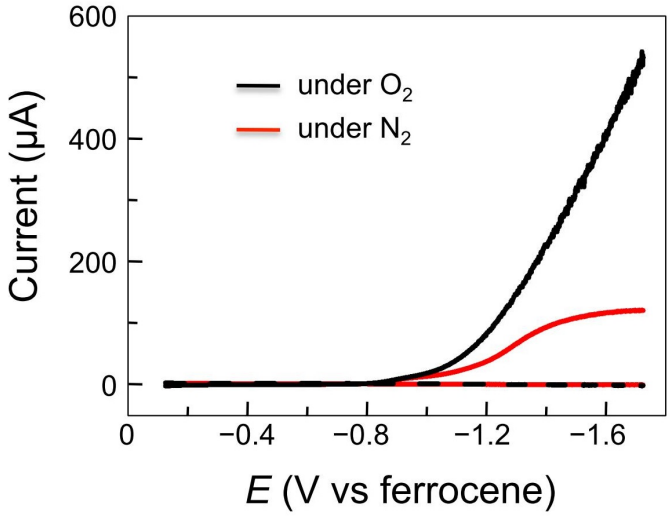

Figure S14. RRDE measurements of 0.1 mM **1** in DMF under O_2 or N_2 with 170 mM of acetic acid. Conditions: −0.72 V (vs ferrocene) ring potential, GC disk (area 0.125 cm^2), Pt ring (area 0.188 cm^2), 50 mV s^{-1} scan rate, 2500 rpm rotation rate, 20 °C.

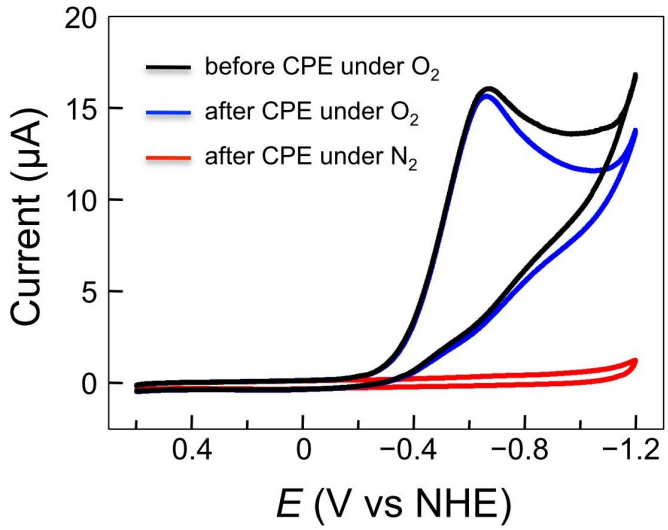

Figure S15. CVs of a freshly cleaned GC electrode under O_2 and a GC electrode after 12-h electrolysis under O_2 and N_2 in 0.1 M pH 7 phosphate buffer.

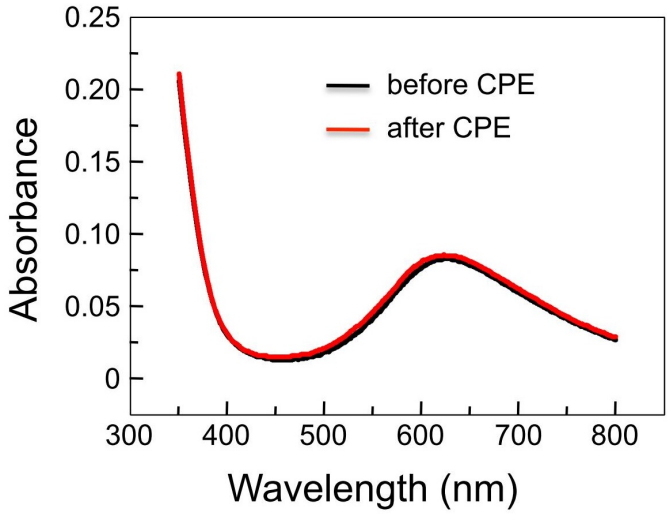

Figure S16. UV-vis spectra of 0.05 mM **1** in 0.1 M pH 7 phosphate buffer before and after 12-h electrolysis under air.

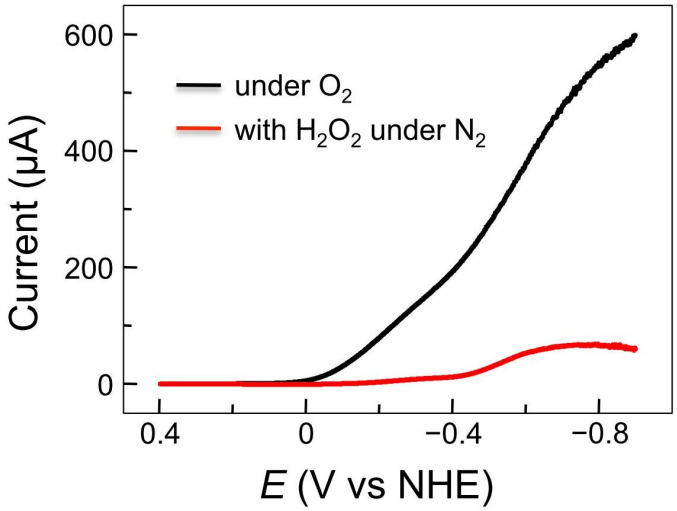

Figure S17. LSVs of 0.05 mM **1** in 0.1 M pH 7 phosphate buffer under O_2 or under N_2 with 1.4 mM of H_2O_2. The currents were corrected by subtracting the background currents. Conditions: GC disk (area 0.125 cm^2), 50 mV s^{-1} scan rate, 2500 rpm rotation rate, 20 °C.

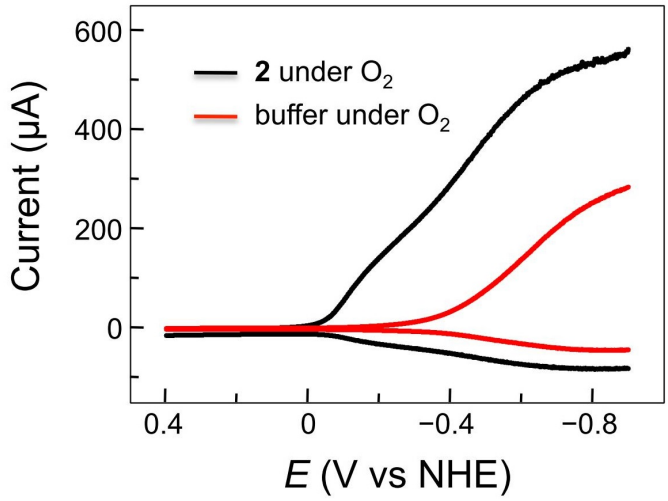

Figure S18. RRDE measurements of 0.1 M pH 7 phosphate buffer with or without 0.1 mM **2** under O_2. Conditions: GC disk (area 0.125 cm^2), Pt ring (area 0.188 cm^2), 50 mV s^{-1} scan rate, 2500 rpm rotation rate, 20 °C.

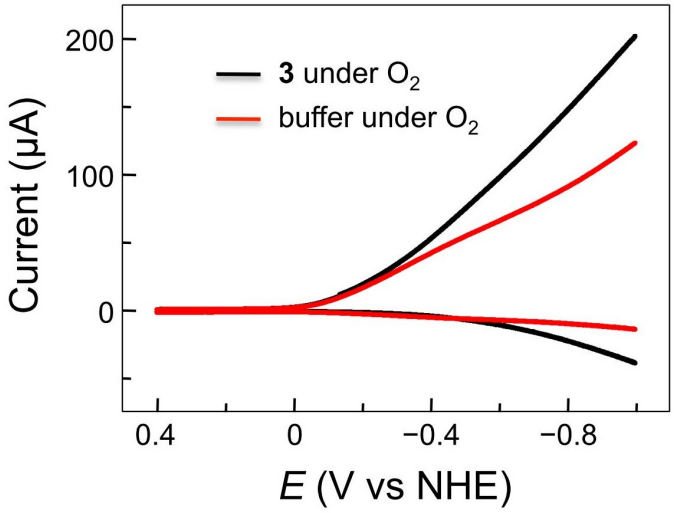

Figure S19. RRDE measurements of 0.1 M pH 7 borate buffer with or without 0.1 mM **3** under O_2. Conditions: GC disk (area 0.125 cm^2), Pt ring (area 0.188 cm^2), 50 mV s^{-1} scan rate, 2500 rpm rotation rate, 20 °C.

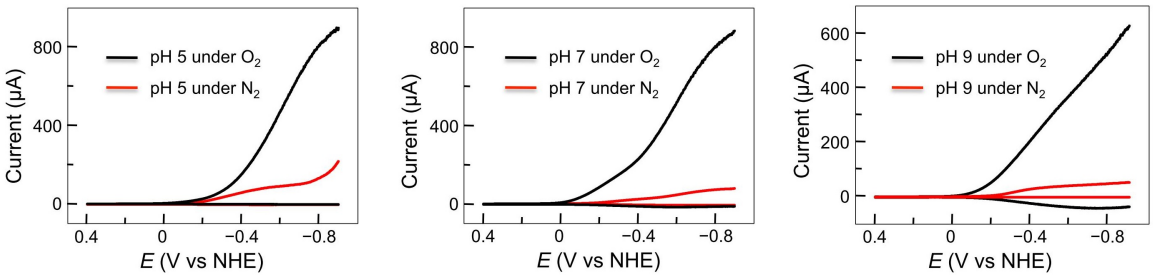

Figure S20. RRDE measurements of 0.05 mM **1** in 0.1 M pH 5 (left), 7 (middle), and 9 (right) phosphate buffers under O_2 and N_2. Conditions: GC disk (area 0.125 cm^2), Pt ring (area 0.188 cm^2), 50 mV s^{-1} scan rate, 2500 rpm rotation rate, 20 °C.

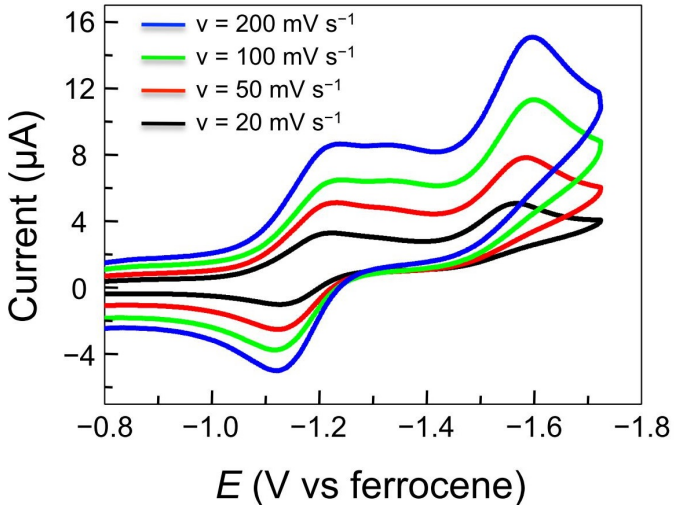

Figure S21. CVs of 0.1 mM **1** in DMF under N_2 with different scan rates. Conditions: GC electrode, 20 °C.

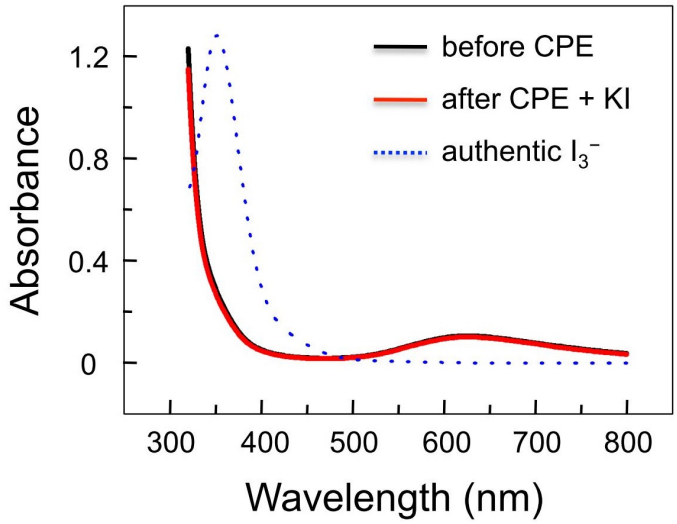

Figure S22. UV-vis spectra of 0.05 mM **1** in 0.1 M pH 7 phosphate buffer before CPE (black), after CPE followed by adding KI (red), and 0.01 mM authentic KI_3 in 0.1 M pH 7 phosphate buffer (dotted blue).

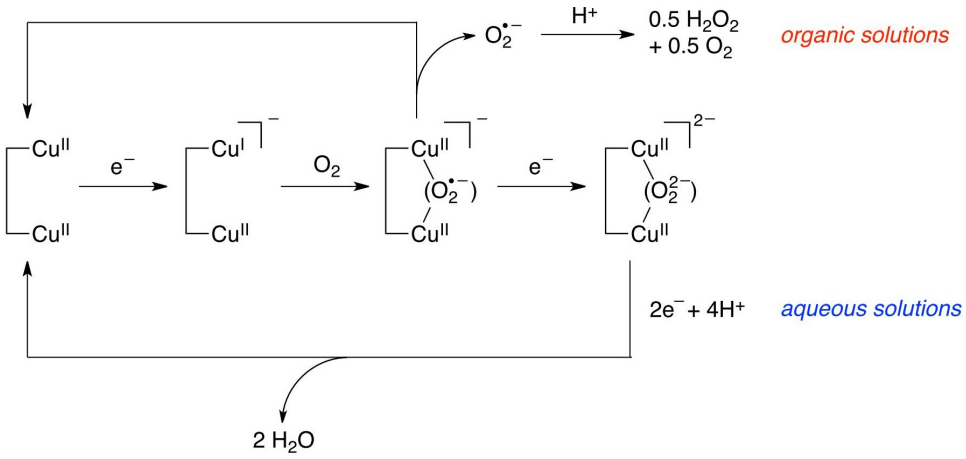

Figure S23. Proposed reaction mechanisms of ORR catalyzed by complex **1** in organic and aqueous solutions.

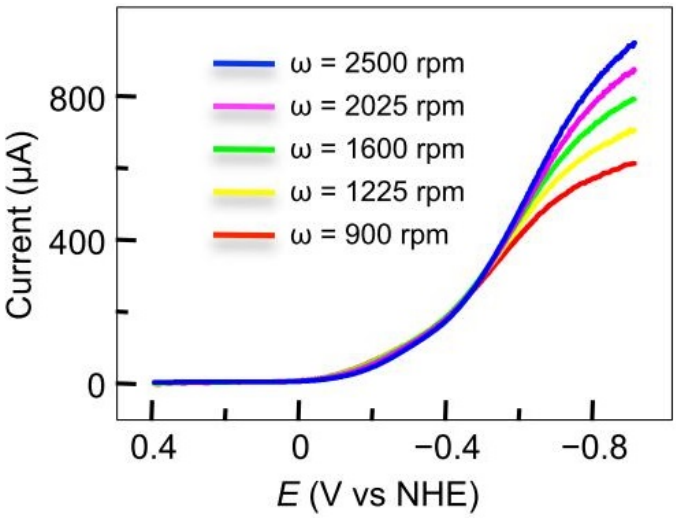

Figure S24. RDE data of **1** under O_2 with various rotation rates.

Table S1. Crystal data and structure refinement parameters for complex **1**.

Complex	**1**
molecular formula	$C_{38}H_{30}Cu_2N_{10}O_{16}$
formula wt. (g mol^{-1})	1009.80
temperature (K)	150(2)
radiation (λ, Å)	0.71073
crystal system	monoclinic
space group	$P2_1/c$
a (Å)	12.5074(4)
b (Å)	17.8257(6)
c (Å)	20.7658(7)
β (°)	97.9380(10)
Volume ($Å^3$)	4585.4(3)
Z	4
ρ_{calcd} (g cm^{-3})	1.463
μ (mm^{-1})	1.006
F(000)	2056
crystal size (mm^3)	0.40 × 0.40 × 0.20
Theta range	2.33 to 28.84°
reflections collected	41202
independent reflections	11897 [R(int) = 0.0431]
Completeness	99.1%
goodness-of-fit on F^2	1.050
final R indices	$R1^a$ = 0.0505
[R > 2σ (I)]	$wR_2{}^b$ = 0.1347
R indices (all data)	$R1^a$ = 0.0723
	$wR_2{}^b$ = 0.1472
largest diff. peak and hole (e $Å^{-3}$)	1.362 and −0.879

$^aR_1 = \Sigma||F_o| - |F_c|| / |F_o|$, $^bwR_2 = \{\Sigma[w(F_o^2 - F_c^2)^2] / \Sigma[w(F_o^2)^2]\}^{0.5}$

References

1. S. H. Liu, Z. Y. Luo and A. D. Hamilton, *Angew. Chem. Int. Ed.*, 1997, **36**, 2678-2680.

2. X. F. Zhang, D. G. Huang, Y. S. Chen and R. H. Holm, *Inorg. Chem.*, 2012, **51**, 11017-11029.

3. *APEX2 v2009*, Bruker AXS, Madison, WI, 2009.

4. G. M. Sheldrick, *SADABS, 2008/1*, University of Göttingen, Göttingen, Germany, 2008.

5. G. M. Sheldrick, *Acta Cryst.*, 1990, **A46**, 467-473.

6. G. M. Sheldrick, *Acta Cryst.*, 2008, **A64**, 112-122.